CrossMark

ORIGINAL ARTICLE

Synthesis and Evaluation of Nonionic Surfactants Derived from Tannic Acid as Corrosion Inhibitors for Carbon Steel in Acidic Medium

Nabel A. Negm[1] · Sayed Abdelkader Ahmed[2] · Emad A. Badr[1] · Mona Abdel Ghani[2] · Mohamed Abd El-Raouf[1]

Abstract Nonionic Schiff base surfactants were synthesized by chemical modification of tannic acid. The surface activities of the synthesized surfactants were determined using surface tension, interfacial tension, and emulsification properties. Thermodynamic parameters of adsorption and micellization of these surfactants showed their tendency towards the two processes with greater predominance of adsorption over micellization. Electrochemical polarization and impedance measurements showed that the surfactants exhibited good tendency towards inhibiting the dissolution of carbon steel in acidic medium. The inhibition efficiencies depend on the chemical structure and concentration of the compounds.

Keywords Nonionic · Surface activity · Adsorption · Micellization · Polarization · Impedance

Introduction

Corrosion inhibitors are compounds added to the medium to decrease the rate of corrosion of metal. Inhibitors are used in closed or circulating systems [1, 2] and are chosen for their effectiveness in protecting the specific metal or different metals in a given system. Halogenated compounds, surfactants, and heterocyclic compounds containing nitrogen, phosphorus, oxygen, and sulfur can inhibit the corrosion of metals [3–6]. Some high molecular weight organic compounds such as proteins and polysaccharides have good corrosion inhibitive properties [7]. Inhibitors prevent the corrosion process and reduce the acid utilization during acid pickling of fabricated metals. The inhibitors' mechanism of action is preceded by electrostatic or chemical interaction between the metal surface and the heteroatoms included in their chemical structures. In spite of the existence of many organic compounds as inhibitors, development of new compounds must be done to achieve more economic, environmentally friendly, and efficient inhibitors [8, 9]. Pure natural compounds can be used as corrosion inhibitors. For example, vanillin was evaluated as an environmentally friendly corrosion inhibitor for aluminum dissolution in acidic medium [10, 11]. Vanillin offers interesting possibilities for corrosion inhibition owing to its environmentally friendly nature [10] and its high solubility in water [12]. The efficiency of pure vanillin was in the range of 80–85 % based on its concentration. The inhibition action of vanillin is attributed to its adsorption on the surfaces through the active centers contained in its structure. Tannic acid is a specific compound of polyphenol tannin. Tannic acid is used in the conservation of ferrous metal objects without the necessity of corrosion products removal from corroded surfaces [13]. Tannic acid is therefore especially useful in anticorrosive protection of objects of heritage. Tannic acid can also be applied in corrosion protection of copper [14], aluminum [15], zinc and nickel [16]. Although tannins can be applied as corrosion inhibitors, sometimes they can increase the acidity of the medium. Thus, modification of the chemical structure of tannic acid can improve the efficiency and applicability of its derivatives as corrosion inhibitors.

Schiff bases are more efficient inhibitors than the corresponding amines. Schiff bases of some aliphatic amines showed excellent inhibition of carbon steel corrosion in

✉ Nabel A. Negm
nabelnegm@hotmail.com

[1] Egyptian Petroleum Research Institute, Nasr City, Cairo, Egypt

[2] Faculty of Science, Beni Suef University, Beni Suef, Egypt

 Springer AOCS

acidic medium, which is of particular interest to petroleum companies [17, 18]. Schiff bases of heterocyclic compounds also showed good inhibition efficiencies for steel in different media [19, 20]. The anticorrosion inhibition efficiency of Schiff bases is attributed to the bonding of imine π electrons with d orbitals of the metal [18, 20]. The aim of this study was to synthesize nonionic surfactants derived from a naturally occurring compound (tannic acid), to study their surface and thermodynamic properties, and to evaluate their ability as inhibitors of the corrosion of carbon steel in acidic medium. The target surfactants were chosen to be environmentally friendly and ideally exhibit higher efficiency as corrosion inhibitors than the reported pure natural compounds.

Experimental Section

Materials

Polyethylene glycols (PEG) of different molecular weight (purity 99.8 %) were purchased from Alfa Aesar, Germany. Vanillin (purity 99 %) and 4-hydroxybenzaldehyde (purity 99.9 %) were obtained from Sigma-Aldrich, Germany. Paraffin oil (a mixture of C_{16}–C_{26} hydrocarbons) was obtained from ADWIC, Egypt.

Synthesis of Tannic Acid–Polyethylene Glycol Esters (T_{1-3})

Tannic acid (0.017 mol, 30 g) was reacted with PEG of different molecular weight (PEG-400, 6.8 g, 0.017 mol; PEG-600, 10.2 g; and PEG-1500, 25.5 g) in the presence of hydrochloric acid (two drops) as a dehydrating agent and 100 mL of xylene as a solvent. The reaction was performed at 138 °C in a 500-mL round-bottom flask equipped with a mechanical stirrer and Dean–Stark condenser. The reaction was stopped after obtaining 0.31 mL of water and cooled. The solvent (xylene) was evaporated under reduced pressure in a closed system oven equipped with a glass trap and mini-vacuum pump. The reaction product was washed with acetonitrile to remove the excess reactants, then with methanol, and dried under vacuum [21]. The obtained products were brown-yellow and waxy, and designated as follows: T_1, tannic acid–PEG-400 (MW 2082 g/mol); T_2, tannic acid–PEG-600 (MW 2282 g/mol); T_3, tannic acid–PEG-1500 (MW 3182 g/mol).

Synthesis of Tannic Acid–Polyethylene Glycol–p-Aminobenzoic Acid Diesters (TA_{1-3})

p-Aminobenzoic acid (0.017 mol, 2.055 g) was reacted with T_{1-3} esters (0.015 mol, 31.23, 34.23, 47.73 g)

individually at 138 °C in the presence of two drops of hydrochloric acid and 100 mL of xylene, as dehydrating agent and solvent, respectively. The reaction was performed in a 250-mL round-bottom flask equipped with a mechanical stirrer and Dean–Stark condenser. The reaction was stopped after obtaining 0.015 mol of water (0.27 mL). The reaction products were washed twice with methanol and dried under vacuum [21]. The solvent was evaporated under reduced pressure in a closed system oven equipped with a glass trap and mini-vacuum pump. The obtained brown waxy esters were designated as follows: TA_1, tannic acid–PEG-400–p-aminobenzic acid (MW 2201 g/mol); TA_2, tannic acid–PEG-600–p-aminobenzic acid (MW 2401 g/mol); TA_3, tannic acid–PEG-1500–p-aminobenzic acid (MW 3301 g/mol).

Synthesis of Vanillin and p-Hydroxybenzaldehyde Schiff Bases of TA_{1-3} Diesters

Vanillin (0.01 mol, 1.52 g) and p-hydroxybenzaldehyde (0.01 mol, 1.22 g) were reacted with the three diesters TA_{1-3} (0.01 mol, 22.01, 24.01, 33.01 g) in the presence of xylene as a solvent at 140 °C, with continuous removal of water during the reaction using a Dean–Stark condenser. The reaction was stopped after obtaining 0.18 mL of water, and then the solvent was removed under reduced pressure. The obtained products were washed with excess methanol and dried under vacuum [22] to obtain six nonionic Schiff bases denoted as follows: V_1, vanillin Schiff base of TA_1; V_2, vanillin Schiff base of TA_2; V_3, vanillin Schiff base of TA_3; H_1, p-hydroxybenzaldehyde Schiff base of TA_1; H_2, p-hydroxybenzaldehyde Schiff base of TA_2; H_3, p-hydroxybenzaldehyde Schiff base of TA_3.

Measurements

Analyses

FTIR spectroscopic analyses were performed using a Genesis FTIR spectrometer, USA.

Surface Tension Measurements

Surface and interfacial tension values were measured by using a Kruss-K6 tensiometer with a platinum ring (precision range ± 0.5 mN/m). Freshly prepared solutions of the synthesized Schiff base nonionic surfactants V_{1-3} and H_{1-3} were prepared with a concentration range of 1×10^{-2} to 5×10^{-5} M in doubly distilled water. Surface tension measurements were performed for the prepared solutions at 25 °C. The measurements were repeated three times and the average was taken for each concentration. Each reading

was measured after 2 min in the measuring cell to allow surface stabilization to be achieved. The measuring cell was made of Teflon to avoid adsorption of surfactant on the cell wall. The platinum ring was washed with diluted acid, acetone, and finally with distilled water after each reading to ensure that accurate values were obtained [23].

Interfacial Tension Measurement

Interfacial tension measurements were performed between light paraffin oil and surfactant solutions with a concentration of 0.1 % by weight at 25 °C. Twenty milliliters of surfactant solution was placed in the measuring cell, and the platinum ring holds in the bottom of the cell. Then, 20 mL of light paraffin oil was placed on the solution surface and the platinum ring was adjusted to locate it at the interfacial surface of the oil–solution system. The interfacial tension value was considered after detachment of the ring from the solution phase to the oil phase. The measurements were repeated three times, each time with a fresh system, and the interfacial tension value was the average of these three readings [24].

Emulsion Stability Measurements

Emulsion stability was measured by placing 25 mL of 0.1 % solution of each surfactant by weight and 25 mL of light paraffin oil in a 100-mL measuring cylinder. The temperature of the cylinder was adjusted to 25 °C. The cylinder was vigorously shaken for 5 min, and the mixture was then allowed to separate. The time required for separation of 20 mL of pure surfactant solution was recorded. Measurements were repeated three times and the time was taken as the average of these readings. Measurements were considered for each surfactant individually, and readings were calculated in minutes [24].

Potentiodynamic Polarization Measurements

Potentiodynamic polarization measurements were performed using a Volta Lab-PGZ-301 (France). A conventional 250-mL cylindrical glass cell equipped by three electrodes was used. A saturated calomel electrode (SCE) and platinum electrode ($2 cm^2$ area) were used as reference and auxiliary electrodes, respectively. The working electrode (carbon steel disc of $0.8 cm^2$) was surrounded with epoxy except the working surface. Potentiodynamic polarization curves were obtained by changing the potential from -200 to $+200$ mV versus open circuit potential (OCP) with the scan rate of $5 mV s^{-1}$. The inhibition efficiency ($\eta\%$) was calculated using the following equation [4, 5].

$$\eta\% = \frac{i_{corr(uninh)} - i_{corr(inh)}}{i_{corr(uninh)}} \times 100$$

where $i_{corr(uninh)}$ and $i_{corr(inh)}$ are the corrosion current densities without and with inhibitors, respectively.

Electrochemical Impedance Spectroscopy (EIS)

Electrochemical impedance spectroscopy measurements were carried out using a Volta Lab, model PGZ-301 (France) and a software program (Voltameter 4) [4]. The measurements were performed using AC signal (10 mV) peak to peak at the OPC in the frequency range of 100 kHz to 10 mHz.

Results and Discussion

Structure

The chemical structures of TA_{1-3} diesters were confirmed by FTIR spectroscopic analysis using a Genesis FTIR spectrophotometer (Mattson, Wisconsin, USA) (Scheme 1).

FTIR spectra of TA_{1-3} showed the following absorption bands: a broad band from 3200 to $3600 cm^{-1}$ centered at $3400 cm^{-1}$ corresponded to hydroxyl and amino groups; two absorption bands at 2920 and $2850 cm^{-1}$ corresponded to symmetric and asymmetric vibration of methylene groups; a band at $1690 cm^{-1}$ corresponded to ester groups, $1190 cm^{-1}$ corresponded to C–N groups, $1029 cm^{-1}$ corresponded to ether groups, and bands at 970 and $730 cm^{-1}$ corresponded to the phenyl groups (see additional data file).

The chemical structures of V_{1-3} were confirmed using FTIR spectroscopic analysis, which showed the following absorption bands: 3100–$3650 cm^{-1}$ broad band centered at $3400 cm^{-1}$ corresponded to hydroxyl groups, two bands at 2920 and $2850 cm^{-1}$ corresponded to CH_2 stretching, $1710 cm^{-1}$ corresponded to ester groups, $1610 cm^{-1}$ corresponded to azomethine groups, $1325 cm^{-1}$ corresponded to C–N groups, $1030 cm^{-1}$ corresponded to ether groups, and 870, 767, 735 and $693 cm^{-1}$ corresponded to phenyl groups (Fig. 1). Similarly, p-hydroxybenzaldehyde Schiff base derivatives (H_{1-3}) showed the listed absorption bands.

Surface Activity of the Synthesized Compounds

Surface Tension and Critical Micelle Concentration

In an aqueous medium, surfactant molecules are adsorbed at the air–water interface such that the hydrophilic part is directed to the water phase and the hydrophobic part is
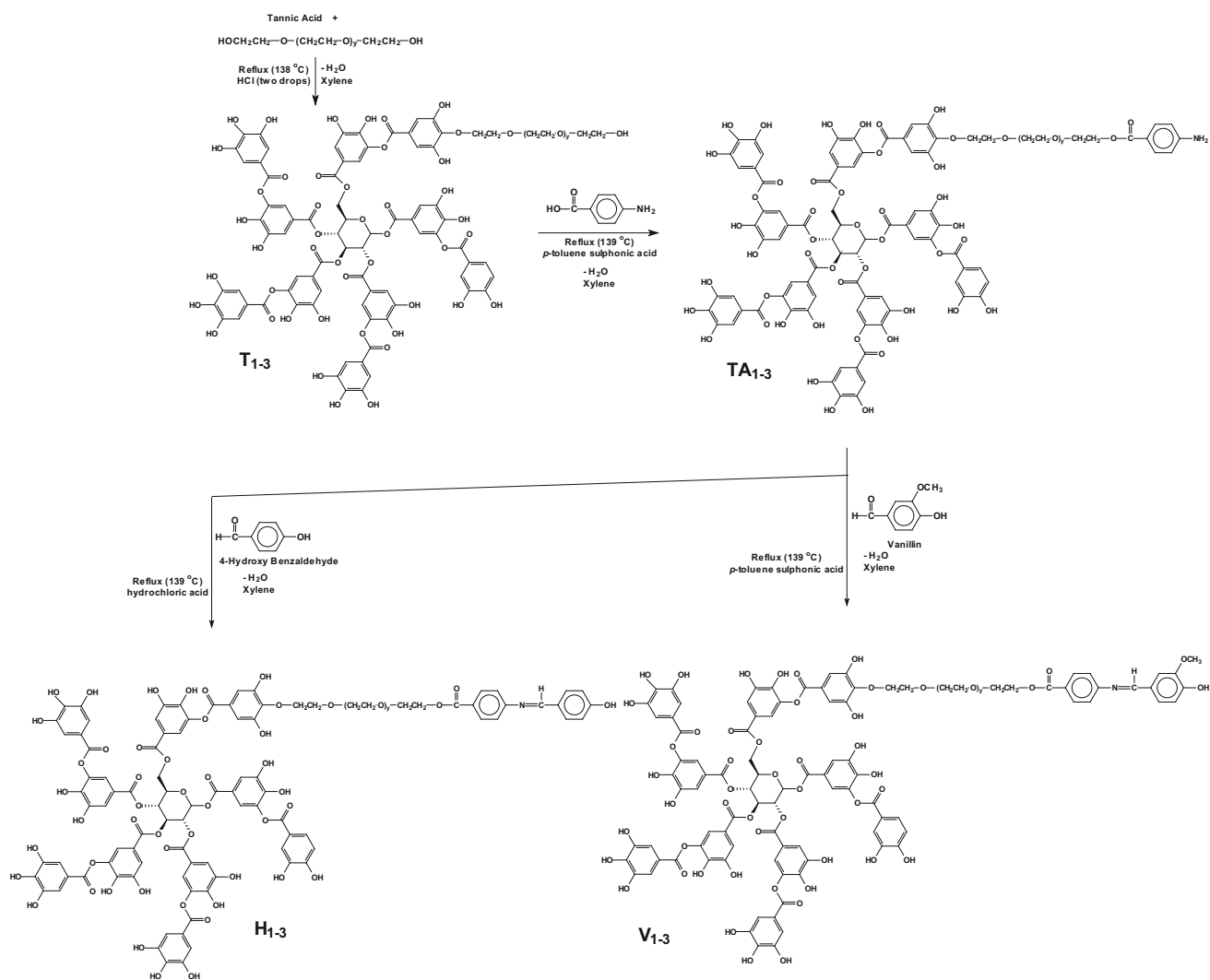
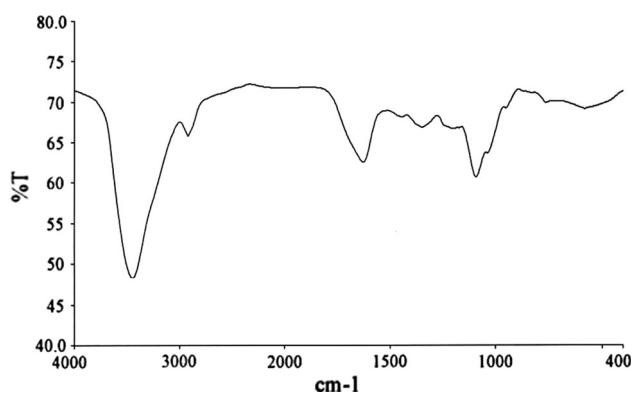**Scheme 1** Synthesis of the nonionic surfactants under study

Fig. 1 IR spectra of V_1 nonionic surfactant

located at the air–water interface. The adsorption of surfactant molecules at the air–water interface decreases the surface tension of the solution, and the gradual increase of the adsorbed surfactants is followed by gradual decrease in the surface tension.

the surface tension. A marked decrease in the surface tension indicates that the surfactant molecules have great tendency towards adsorption at the air–water interface.

The surfactants under consideration are nonionic surfactants owing to the presence of nonionic PEG species, in addition to the huge number of hydroxyl groups attached to the phenyl groups, in their chemical structures as hydrophilic groups. Their chemical structure has no fully positively or negatively charged head groups. The hydrophobic groups are the organic part obtained from the reaction of vanillin or 4-hydroxybenzaldehyde with p-aminobenzoic acid. Figure 2 shows the variation of surface tension vs – log concentration relationships of the synthesized nonionic surfactants ($V_{1–3}$) for $H_{1–3}$ in their solutions (see additional data file). The relation showed two characteristic regions: the premicellar region in which the surface tension values decrease with increasing surfactant concentration and the postmicellar region in which the surface tension stays
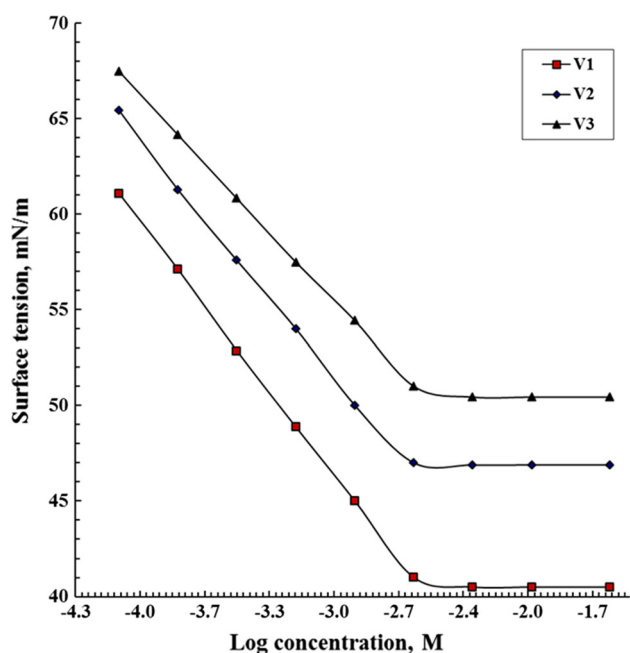
Fig. 2 Surface tension versus minus log concentration of V_1, V_2, and V_3 Schiff base nonionic surfactants at 25 °C

almost constant with increasing concentration of each surfactant [25]. Intersection of the two regions determines the concentration at which the micelles form (the critical micelle concentration, CMC) [26].

The PEG chain length has an important effect on the surface tension values of the surfactants in their solutions. Surfactant molecules with shorter PEG chains have lower surface tension values in the solutions compared to the surfactant molecules with longer PEG chains. Surfactants with longer PEG chains (V_3 and H_3) have the highest surface tension values. In contrast, surfactant molecules with PEG-400 (V_1 and H_1) have the lowest surface tension values (Fig. 2).

Surfactant molecules with shorter PEG chains (V_1, H_1) are rapidly and strongly adsorbed at the air–water interface. That is due to the hydrophobicity of their molecules. On the other hand, increasing the PEG chain length to 600 and 1500 g/mol (V_{2-3}, H_{2-3}) increases the surface tension values of the surfactant solutions considerably, compared

to V_1 and H_1 surfactants. The surface tension–concentration profiles show that the surface tension values of the synthesized surfactants are relatively low compared to the conventional nonionic surfactants [27].

The CMC values of the synthesized nonionic surfactants were extracted from Fig. 2 and are listed in Table 1. They ranged between 2.15 and 2.71 mM for derivatives containing PEG-400 chains (V_1, H_1) and between 2.71 and 5.83 mM for derivatives containing PEG-1500 chains (V_3, H_3). The main factor influences the CMC values of these surfactants is the PEG chain length within similar series (H_{1-3} or V_{1-3}). Increasing the PEG chain length from 400 to 600 g/mol has a noticeable influence on the CMC values. Surfactant molecules containing short PEG chains (V_1, H_1) are more hydrophobic than surfactant molecules with longer PEG chains (V_3, H_3), which are more hydrophilic [28]. The hydrophobicity of molecules with short PEG chains increases the adsorption of surfactant molecules at the air–water interface, which decreases the CMC values.

The side chains attached to the surfactant molecules have a considerable influence on the CMC values. 4-Hydroxybenzaldehyde interacts with the aqueous phase via the formation of two types of hydrogen bonds: the first involves the PEG chain and the second involves the hydroxyl groups of the benzaldehyde ring and tannic acid moiety. On the other hand, vanillin-derived nonionic surfactants have a third type of hydrogen bonding via the methoxy group on the vanillin moiety. As a result, the adsorption of vanillin-derived surfactants is expected to be planar on the aqueous phase (well-arranged molecules at the interface) compared with the 4-hydroxybenzaldehyde-derived surfactants which will be tilted as a result of the adsorption sites being located in one geometrical line (randomly arranged molecules at the interface). The well-arranged vanillin derivative increases its concentration at the interface. As a result, the surface concentration increases which decreases the CMC values (Table 1).

Surfactant molecules in the aqueous medium experience two balanced forces. The first is the repulsion exerted by the polar phase on the hydrophobic chains (due to the hydrophobic effect), and the second is the attraction between the water molecules and the partially charged

Table 1 Surface activity of the synthesized surfactants in their solutions at 25 °C

Surfactant	CMC (mM)	γ_{cmc} (mN m^{-1})	π_{cmc} (mN m^{-1})	Pc_{20} (mM)	$-\partial\gamma/\partial\log C$	Γ_{max} (mol cm^{-2} × 10^{-10})	A_{min} (nm^2)
H_1	2.71	42	29.8	0.45	11.99	4.84	34.3
H_2	3.03	45	26.8	0.86	10.78	4.35	38.2
H_3	5.83	47	24.8	2.24	8.85	3.59	46.2
V_1	2.15	43.5	28.3	0.48	13.36	5.93	27.9
V_2	2.32	47.0	24.8	1.16	12.29	4.96	33.5
V_3	2.71	50.5	21.3	2.51	10.9	4.39	37.8

nonionic chains and the hydroxyl groups of phenyl moieties (due to the hydrophilic effect). The former effect suppresses the adsorption of molecules at the air–water interface, whereas the latter effect increases the solubility of the surfactant molecules in the aqueous bulk via hydrogen bond formation between the water molecules and the electronegative oxygen atoms within PEG chains and hydroxyl groups. The effect of hydrophobicity of surfactant molecules in the solution is overcome by two ways. The first is the adsorption of more hydrophobic surfactant molecules at the air–water interface. The second is the aggregation of surfactant molecules in the bulk solutions to form micelles.

The γ_{cmc} value is defined as the surface tension of the surfactant solution at the CMC [27]. γ_{cmc} illustrates the surface activity of the surfactant solutions at the interface. This value determines the lowest surface tension value which can be achieved by the surfactant solution. Decreasing γ_{cmc} values indicates the high surface activity of the surfactants in their solutions. The lowest γ_{cmc} values were obtained with V_{1-2} and H_{1-2}; furthermore, vanillin-derived surfactants (V_{1-3}) have higher values than the corresponding 4-hydroxybenzaldehyde derivatives (H_{1-3}) (Table 1). The depression in γ_{cmc} values indicates the extent of surfactant molecules adsorbed at the solution interface.

Effectiveness (π_{cmc}) and Efficiency (Pc_{20})

The difference between the surface tension values of doubly distilled water and the surfactant solution at the CMC is defined as the effectiveness (π_{cmc}). π_{cmc} describes the depression in surface tension at surface saturation conditions [28]. π_{cmc} is useful in comparing between surfactants which have similar head groups. Surfactants with higher π_{cmc} values have a greater tendency to adsorb at the air–water interface than ones with lower π_{cmc} values. Comparing π_{cmc} values of V_{1-3} or H_{1-3} surfactants in Table 1 reveals that the sequence of surfactants towards adsorption at the interface is in the following order: $V_1 > V_2 > V_3$ and $H_1 > H_2 > H_3$.

The efficiency, Pc_{20}, describes the concentration of surfactant solution which reduces the surface tension of doubly distilled water by 20 mN/m. It is helpful in comparing between surfactants having different head groups. It is clear that the 4-hydroxybenzaldehyde derivatives (H_{1-3}) are more pronounced in decreasing the surface tension than vanillin derivatives (V_{1-3}). Based on π_{cmc} and Pc_{20} values, it can be reported that H_1, H_2, V_1, and V_2 surfactants have greater tendencies towards adsorption at the air–water interface than H_3 and V_3 surfactants.

Maximum Surface Concentration (Γ_{max})

The slope of the premicellar region in the surface tension–concentration profile is called the surface pressure. The surface pressure ($\partial\gamma/\partial\log C$) determines the change in the surface tension of the surfactant solution with infinitesimal change in the surfactant concentration. Its value is a direct indication of the adsorption tendency of the surfactant molecules at the air–water interface. Increasing the surface pressure indicates the increasing of the surfactant molecules adsorption tendency at the air–water interface [24, 25, 29]. Data in Table 1 showed that V_1, V_2, H_1, and H_2 surfactants, respectively, have higher surface pressures than V_3 and H_3 surfactants. That reflects the higher tendency of V_1, V_2, H_1, and H_2 surfactants towards adsorption at the interface than V_3, and H_3 surfactants.

The surface pressure values can be used to calculate the maximum surfactant concentration Γ_{max} of different surfactants at the interface of their solutions as follows [27]:

$$\Gamma_{max} = (\partial\gamma/\partial\log C)/(2.303nRT)$$

where Γ_{max} is the maximum surface concentration at the saturation condition, n is the number of ionic species in the solution ($n = 1$ in case of nonionic surfactant), R is the universal gas constant, and T is the absolute temperature; the obtained results are listed in Table 1.

The maximum surface excess is the concentration of surfactant per unit area at the interface. The adsorption of surfactant molecules at the interface is calculated numerically in terms of concentration by Γ_{max}. The values of Γ_{max} in Table 1 vary over a narrow range within similar series and widely within different series. Within similar series, Γ_{max} ranged between 4.39×10^{-10} and 5.93×10^{-10} mol/cm^2 for V_{1-3} and ranged between 3.59×10^{-10} and 4.84×10^{-10} mol/cm^2 for H_{1-3}, which indicates the high adsorption tendency of the different surfactants at the interface. The higher surface concentration at the interface is related to the pumping of surfactant molecules to that interface. The adsorption of surfactant molecules at the air–water interface is decreased by increasing the hydrophilicity of the molecules and increased by increasing the hydrophobicity of the chains. On the other hand, higher surface concentration is related to the stability of the formed monolayer at this interface. Vanillin derivatives (V_{1-3}) have lower surface pressure than H_{1-3} owing to the presence of methoxy groups in their structure. The presence of methoxy groups increases the attachment of V_{1-3} surfactant molecules to the aqueous phase, which decreases the adsorption of molecules at the interface. At the interface, the adsorbed monolayer of V_{1-3} surfactant molecules is compact owing to the overlapping

between the polar groups in their chemical structure. That compactness is less pronounced in H_{1-3} surfactant molecules as a result of the presence of only hydroxy groups in their chemical structure. The difference in Γ_{max} values listed in Table 1 is not pronounced, indicating the slight effect of the methoxy group on the adsorption of V_{1-3} at the interface relative to H_{1-3} surfactant molecules. The adsorption tendency of the surfactants at the interface increases their applicability in several interfacial applications including emulsification, foaming, wetting, and corrosion inhibition. The synthesized surfactants were expected to adsorb at the metal surface and act as corrosion inhibitors owing to the presence of the various polar groups in their chemical structure. In addition, the phenyl and azomethine groups in their chemical structures can form bonds with the metal surface by overlapping between the π electrons and the p electrons of the iron in carbon steel.

Minimum Surface Area (A_{min})

The average area occupied per surfactant molecule at the interface at saturation conditions (A_{min}) was calculated using the following formula (N_{avog} is Avogadro's number) [29]:

$$A_{min} = 1/(G_{max}.N_{avog})$$

Values listed in Table 1 indicate that the surfactant molecules are located in a semiplanar position at the interface [29]. Furthermore, increasing the PEG chain length has a minor effect on the A_{min} values of the different surfactants. The influence of the vanillin and 4-hydroxybenzaldehyde moieties on A_{min} values is more pronounced. Vanillin-derived surfactants V_{1-3} occupy a smaller area at the interface than the 4-hydroxybenzaldehyde-derived surfactants, H_{1-3}. That can be simply related to the presence of the polar groups in the two moieties. The obtained values of A_{min} were comparable to our previous work for nonionic surfactants based on tannic acid [30]. A_{min} values of five substituted tannic acid nonionic surfactants were comparable to our values when considering one substituent on the tannic acid moiety.

Thermodynamic Properties of the Synthesized Surfactants

The standard free energy of micellization (ΔG_{mic}) is the energy loss in the system due to the transfer of one mole of surfactant molecule to the bulk of the solution during the micellization process and can be calculated using the Gibbs equation as follows [29]:

$$\Delta G_{mic} = 2.303nRT(\log CMC)$$

where R is the universal gas constant (8.314 kJ/mol) and T is the absolute temperature (K).

The adsorption free energy (ΔG_{ads}) is the energy loss in the system due to the adsorption of surfactant molecules (1 mol) at the air–solution interface and is given using the following equation [29]:

$$\Delta G_{ads} = \Delta G_{mic} - (0.6 \times \pi_{cmc} \times A_{min})$$

where ΔG_{mic} is the standard free energy of micellization in kJ mol^{-1}, π_{cmc} is the effectiveness (mN/m), and A_{min} is the average area occupied by a surfactant molecule at the solution interface (nm^2).

The thermodynamics of adsorption and micellization processes of the synthesized surfactants were calculated according to the two aforementioned equations [29].

The thermodynamics of both adsorption and micellization processes determine the affinity of surfactant towards adsorption at the interface, or micellization in their solutions. The negative values of ΔG_{mic} and ΔG_{ads} indicate that the adsorption of surfactant molecules at the interface and the micellization in the bulk of the solution occurred spontaneously (Table 2). Furthermore, the narrow difference between these two values indicates the presence of equilibrium between the adsorbed molecules at the interface and the micellized molecules in the bulk. Data in Table 2 show that the free energies of adsorption are more negative than those of micellization. This provides evidence for the preferential tendency of the prepared surfactants towards adsorption at the air–water interface than micellization in the bulk of their solutions (i.e., the predominance of adsorption process over micellization). The thermodynamic evaluation of the adsorption and

Table 2 Emulsification, interfacial properties, and thermodynamic parameters of V_{1-3} and H_{1-3} surfactants in their solutions at 25 °C

Surfactant	ΔG_{ads} (kJ mol^{-1})	ΔG_{mic} (kJ mol^{-1})	Emulsion stability (min)	Interfacial tension (mN/m)
H_1	−15.91	−14.20	70.25	26
H_2	−15.53	−13.94	2.40	24
H_3	−14.78	−12.36	1.05	23
V_1	−15.28	−14.76	37.25	26
V_2	−14.89	−14.58	3.15	23
V_3	−14.42	−14.20	1.30	22

micellization processes of the different surfactants was performed according to the standard free energies (ΔG_{ads} and ΔG_{mic}) of these two processes, respectively [22].

Emulsion Stability

Emulsion formation technology is very important in several applications, especially in cosmetics, drug formulations, and paints. The emulsification by surfactants is one of the most important surface properties at the interface. The emulsification tendency in some cases is important for the formation of stable emulsions, e.g., in solubilization, emulsification processes, cosmetics and drug formulations; whereas, in some applications emulsification is not favorable, e.g., especially in petroleum applications including demulsification and corrosion inhibition. The emulsification powers of the synthesized surfactants were determined as the time required to break down the emulsion formed between surfactant solution and paraffin oil. Table 2 lists the emulsification properties of the synthesized surfactants in the presence of light paraffin oil. The stability of the oil–water emulsions are mainly dependent on the chemical structure of the emulsifier used (surfactant), pH of the medium, and the temperature. The emulsification powers of the surfactants are dependent on the nonionic chain length. The synthesized surfactants showed different responses towards the emulsion stabilization. Surfactants containing short PEG chains (H_1 and V_1) exhibit moderate emulsion stability ranging between 70.25 and 37.25 min. Surfactants containing longer PEG chains (H_2 and V_2) exhibit considerably lower emulsion stability of between 2.40 and 3.15 min. The lowest stability of the formed emulsions was obtained in presence of H_3 and V_3 surfactants. The relatively low stability of emulsion formed using H_{1-3} and V_{1-3} was comparable to the emulsions formed by conventional nonionic surfactants, e.g., Tween-20 or Tween-40 [29], which provide stable emulsions for more than 2 days. That behavior predicts the applicability of these surfactants as corrosion inhibitors in oil fields owing to the lack of risk of stable emulsion formation, which is undesirable in the chemicals used there.

Interfacial Tension

Interfacial tension is a property that determines the ability of compounds to locate at the interface between the oil and the water phase. The driving force of surfactant molecules to adsorb at the interface (boundary surfaces) is to decrease the free energy at these boundaries. That decrease can be observed from the interfacial energy values. Interfacial tension is expressed instead of interfacial free energy per unit area. The tendency of surfactant molecules towards accumulation at the interfaces is a unique property of

surfactants [31]. The interfacial tension values of the synthesized surfactants (H_{1-3}, V_{1-3}) ranged between 22 and 26 mN/m at 25 °C. The relatively high values of the synthesized surfactants compared to Tween-20 or Tween-40 (12, 9 mN/m) indicate their low tendency to locate at the oil phase. This phenomenon is suitable when evaluating these surfactants in oil and water environments, e.g., corrosion inhibition of petroleum equipment [13, 14, 16]. The presence of water and oil in the same environment risks the formation of stable emulsion when the interfacial tension values of the surfactants are low. In the case of the synthesized surfactants, there is no risk of stable emulsion formation when these compounds are used in different applications. Increasing the hydrophilic chain length (PEG chains) from 9 to 34 units decreases the interfacial tension of vanillin derivatives V_{1-3} from 26 to 22 mN/m, whereas in the case of H_{1-3}, the interfacial tension values decreased from 26 to 23 mN/m at 25 °C (Table 2).

Corrosion Inhibition Evaluation

Potentiodynamic Polarization Spectroscopy

The current–potential relationship (cathodic and anodic) for carbon steel corrosion in 1 N H_2SO_4 in the presence of 5000–500 ppm by weight of V_{1-3} inhibitors at 25 °C is shown in Fig. 3 for H_{1-3} (see additional data file). The electrochemical polarization parameters of cathodic and anodic Tafel slopes (β_c, β_a), corrosion current density (i_{corr}), potential of corrosion (E_{corr}), and inhibition efficiency ($\eta\%$) obtained from this figure are listed in Table 3. The potential of corrosion of the unprotected carbon steel was −492.9 mV compared with the saturated calomel
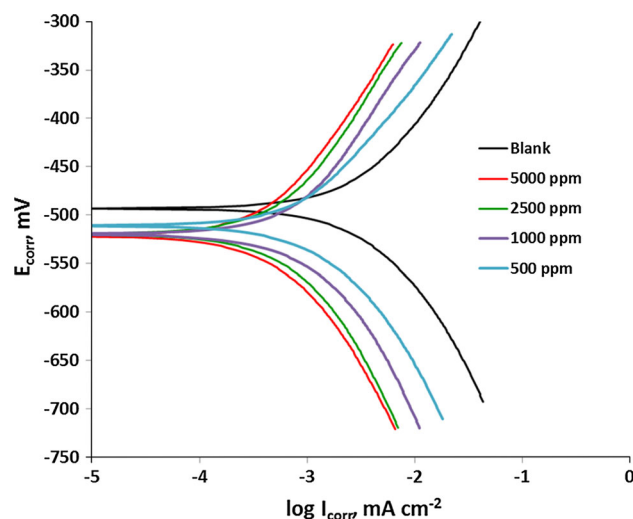

Fig. 3 Polarization curves of carbon steel in the presence of 5000–500 ppm by weight of V_1 nonionic surfactant at 25 °C

Table 3 Electrochemical polarization parameters of carbon steel corrosion in the presence of different concentrations of V_{1-3} and H_{1-3} nonionic surfactants

Inhibitor	Concentration (ppm by weight)	$-E_{corr}$ (mV)	I_{corr} (mA/cm^2)	β_a (mV)	β_c (mV)	θ	η %
Blank	0	492.9	1.99	206.7	201.5	–	–
V_1	5000	521.4	0.208	245.7	243.4	0.90	89.5
	2500	519.6	0.201	239.2	234.0	0.87	86.5
	1000	519.9	0.311	221.9	215.6	0.79	79.1
	500	510.9	0.423	190.5	202.4	0.72	71.6
V2	5000	511.4	0.190	250.6	248.3	0.90	90.5
	2500	529.6	0.239	244.0	238.7	0.88	87.5
	1000	529.9	0.318	226.3	219.9	0.84	84.3
	500	520.9	0.478	194.3	206.4	0.76	76.4
V3	5000	523.4	0.179	253.1	250.7	0.91	91.0
	2500	522.6	0.199	246.4	241.0	0.90	90.0
	1000	529.9	0.279	228.6	222.1	0.86	86.3
	500	523.9	0.398	196.2	208.5	0.80	80.0
H_1	5000	509.2	0.297	246.2	225.0	0.80	80.1
	2500	510.7	0.393	237.9	213.7	0.74	73.6
	1000	505.6	0.511	230.2	210.4	0.69	68.7
	500	503.3	0.875	228.2	205.6	0.59	59.3
H2	5000	519.2	0.358	251.1	229.5	0.82	81.6
	2500	520.7	0.418	242.7	218.0	0.79	79.1
	1000	505.6	0.478	234.8	214.6	0.76	76.4
	500	503.3	0.677	232.8	209.7	0.66	65.8
H3	5000	509.2	0.318	253.6	231.8	0.84	84.3
	2500	510.7	0.398	245.0	220.1	0.80	80.4
	1000	505.6	0.438	237.1	216.7	0.78	78.4
	500	503.3	0.557	235.0	211.8	0.72	71.8

electrode, while the corrosion current recorded a very high value of 1.991 mV. That indicates the high corrosion extent of the carbon steel in the acidic medium with high tendency towards cathodic polarization at 201.5 mV compared to the saturated calomel electrode. The corrosion potential of the carbon steel in the presence of the different inhibitors increased, indicating the protection of the metal surface as a result of the presence of the inhibitors in the medium. The corrosion currents were decreased considerably by the addition of the inhibitors to lower values of 0.208, 0.190, 0.179, 0.297, 0.358, and 0.318 mA cm^{-2} at 5000 ppm by weight of V_{1-3} and H_{1-3}, respectively. The values of the corrosion currents were used to determine the surface coverage (θ) of the carbon steel by the inhibitor molecules using the following equation [32]:

$$\theta = \left(i_{corr(uninh)} - i_{corr(inh)}\right)/\left(i_{corr(uninh)}\right)$$

where $i_{corr(uninh)}$ and $i_{corr(inh)}$ are the corrosion current densities in the presence and absence of the different inhibitors. These values were used to determine the corrosion inhibition efficiencies of the different inhibitors at 400 ppm according the following equation [4]:

$$n\% = \left[\left(i_{corr(uninh)} - i_{corr(inh)}\right)/\left(i_{corr(uninh)}\right)\right] \times 100$$

At 5000 ppm by weight, the values of i_{corr} in the case of V_3 and H_3 (0.179, 0.318 mA cm^{-2}) are smaller than those of V_{1-2} and H_{1-2} (Table 3). V_3 and H_3 thus exhibit higher inhibition efficiencies (91.0, 84.3 %) than the other inhibitors in 1 N H_2SO_4 at 25 °C. It is apparent from the polarization profile that both anodic and cathodic corrosion reactions of carbon steel electrode were inhibited after the addition of the different inhibitors to the acidic solution. Furthermore, the inhibition became more noticeable by increasing the inhibitor concentration from 500 to 5000 ppm by weight. This behavior indicates that the addition of the inhibitors lessens the anodic dissolution of iron and also retards the reduction of hydrogen ions (hydrogen evolution) [32]. The cathodic current–potential curves (Fig. 3) gave rise to parallel lines indicating that the presence of inhibitors did not alter the hydrogen evolution mechanism and the reduction of H^+ ions at the carbon steel surface takes place mainly through a charge transfer mechanism [33]. The cathodic current densities decreased dramatically by increasing the inhibitor concentrations, which reveals that the addition of the inhibitors does not

change the cathodic hydrogen evolution mechanism. The suppression of the cathodic process can be attributed to the covering of inhibitor monolayer on the cathodic sites of the carbon steel [34–36]. In the initial stage of the anodic polarization, the corrosion current densities increased slowly and the anodic polarization was enhanced predominantly with the polarization potential shifting positively. That shows the adsorption rate is higher than the desorption rate of the inhibitor molecules on carbon steel surface, and the adsorption process controls the anodic reaction [37]. The polarization behavior showed similar appearance, which implies that the inhibitor molecules are thoroughly adsorbed from the solution to the carbon steel surface and their inhibition effect is increased by increasing the concentration [9, 38]. Increasing of inhibitor concentration results in a reduction in the corrosion current densities and an increase in $\eta\%$, which suggests that the protective film adsorbed on the metal surface tends to be more complete at higher inhibitor concentrations. Furthermore, increasing the number of ethylene glycol units in the inhibitors decreased the corrosion current density (i_{corr}) considerably. The inhibition efficiencies increased by increasing the polymerization extent in the following order: $V_3 > V_2 > V_1 > H_3 > H_2 > H_1$. The inhibitors are classified as cathodic or anodic type when there is a shift in corrosion potential higher than 85 mV compared to the corrosion potential in the absence of inhibitors [9]. However, the displacement of E_{corr} is less than 85 mV for all the studied inhibitors. Therefore, these inhibitors can be classified as mixed-type inhibitors [39, 40]. Mixed-type inhibitors retard both cathodic and anodic reactions of the corrosion process. Moreover, the values of the anodic and cathodic Tafel slopes showed no obvious changes with the addition of the inhibitors. That suggests the adsorption of inhibitor molecules occurs first on the carbon steel surface. This then successively hinders the corrosion process by blocking the reactive sites on the carbon steel surface without changing the corrosion reaction mechanism [4, 22, 41]. The surface coverage values showed an increasing trend with increasing the inhibitor concentration from 500 to 5000 ppm by weight (Table 3). That causes an increase in the adsorbed inhibitor molecules on the metal surface, which increases the inhibition efficiencies of the inhibitors. Increasing the inhibition efficiencies accompanied by increasing the inhibitors concentration can be attributed to the increase of the adsorbed layer thickness [41].

Electrochemical Impedance Spectroscopy (EIS)

Electrochemical impedance spectroscopy (EIS) measurements were used to study the corrosion behaviors of carbon steel in 1 N H$_2$SO$_4$ solution in the absence and the presence of 500–5000 ppm by weight of V$_{1–3}$ and H$_{1–3}$ inhibitors
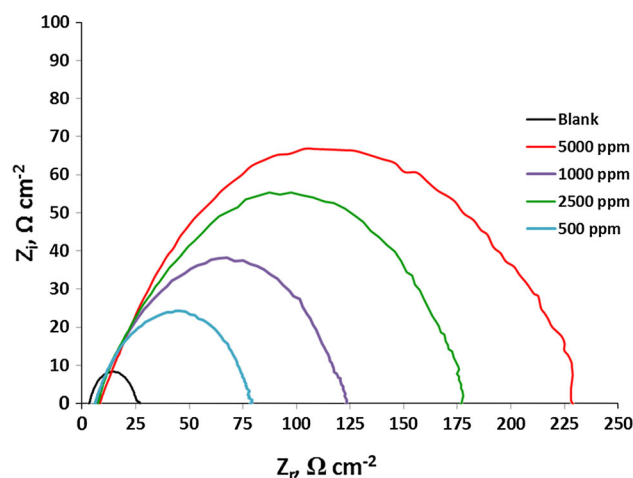

Fig. 4 Electrochemical impedance curves of carbon steel in the presence of 5000–500 ppm by weight of V$_1$ nonionic surfactant at 25 °C

(Fig. 4). The charge transfer resistance (R_{ct}) values were calculated on the basis of the differences between impedance values at higher and lower frequencies as follows [40]:

$$C_{dl} = 1/\omega R_{ct}, \quad \omega = 2\pi f_{max}$$

where ω is the angular frequency (in rad/s) and f_{max} is the maximum frequency.

The recorded EIS spectrum for carbon steel in 1 N H$_2$SO$_4$ at 25 °C in the absence and in the presence of 500–5000 ppm by weight of V$_{1–3}$ and H$_{1–3}$ nonionic surfactants showed one depressed capacitive loop (illustrated for V$_1$ in Fig. 4). The depressed semicircle with the center under the real axis is attributed to the roughness and inhomogeneities of the metal surface [42–44]. Inspection of Fig. 4 reveals that the addition of the inhibitors increases the capacitive loop diameter without affecting their characteristic features. This indicates the strengthening of the formed inhibitive film which is responsible for the inhibition action of these inhibitors. The protective film is formed as a result of adsorption of inhibitor molecules on the carbon steel surface without changing the mechanism of the corrosion process [27]. In fact, the presence of inhibitors enhances the value of the transfer resistance in the acidic solutions [32]. The EIS study confirms that the tested inhibitors are efficient as corrosion-retarding compounds. Table 4 lists the impedance parameters derived from the ESI measurements and shows that the values of R_{ct} increase with increasing inhibitor concentration. This behavior is attributed to the adsorption of V$_{1–3}$ or H$_{1–3}$ molecules on the carbon steel surface, which resulted in increasing their corrosion inhibition efficiency in the acidic solution [34]. The impedance diagram showed that the corrosion of carbon steel is mostly controlled by the charge

Table 4 Electrochemical impedance parameters of carbon steel corrosion in the presence of different concentrations of V_{1-3} and H_{1-3} nonionic surfactants

Inhibitor	Concentration (ppm by weight)	R_{ct} (Ω cm^{-2})	h (%)	C_{dl} (uF cm^{-2})	q
Blank	0	17.5	–	175.6	–
V_1	5000	221.7	92.1	109.7	0.92
	2500	160.7	89.1	90.44	0.89
	1000	116.7	85	86.15	0.85
	500	72.5	75.9	74.57	0.76
V2	5000	241.7	92.8	137.1	0.93
	2500	175.2	90	113.1	0.9
	1000	127.2	86.2	107.7	0.86
	500	79	77.9	93.2	0.78
V3	5000	250.5	93	175.5	0.93
	2500	181.6	90.4	144.7	0.9
	1000	131.9	86.7	137.8	0.87
	500	81.9	78.6	119.3	0.79
H_1	5000	97.1	82	233.9	0.82
	2500	78.9	77.8	144.5	0.78
	1000	66.7	73.8	138.5	0.74
	500	46.5	62.4	125.7	0.62
H2	5000	105.8	83.5	292.4	0.83
	2500	86	79.7	180.6	0.8
	1000	72.7	75.9	173.1	0.76
	500	50.7	65.5	157.1	0.65
H3	5000	109.7	84.1	374.2	0.84
	2500	89.2	80.4	231.2	0.8
	1000	75.4	76.8	221.6	0.77
	500	52.5	66.7	201.1	0.67

transfer process. The double-layer capacitance, C_{dl}, decreased in the presence of the studied inhibitors. This decrease is due to the increase in the thickness of the electrical double layer and/or the reduction of local dielectric constant, which suggests that the inhibitors achieve their action by the adsorption on the metal–solution interface [45]. Thus, the change in C_{dl} values is due to the gradual replacement of adsorbed water molecules on the carbon steel surface by the inhibitor molecules and consequently decreases the dissolution process of the metal [46–48]. The adsorption of these inhibitors on the metal surface includes overlapping between the PEG chains and the positive centers on the metal surface via chemical and/or physical attraction.

Synthesized Inhibitors Versus Commercial Nonionic Corrosion Inhibitors

Water-soluble nonionic Rosen surfactants (cheap commercial corrosion inhibitors) showed inhibition efficiency against corrosion of carbon steel in 1 N HCl in the range of 73–88 % at high concentrations [49]. Commercial nonionic ethoxylated fatty acid surfactants Co(EO)$_n$ ($n = 20$, 40, and 80) [50] were evaluated as corrosion inhibitors using low carbon mild steel at 25 °C in 0.25 M H$_2$SO$_4$. The efficiencies of these inhibitors ranged between 85 and 90 %. Tween is one of the most common commercial nonionic surfactants which can be used as a corrosion inhibitor. Tween 80, 60, 40, and 20 were tested as inhibitors for corrosion of nickel in 1 M H$_2$SO$_4$ solution [51]. The efficiencies varied depending on the PEG chain length in the range of 89.54–94.36 %. Polysorbate is another type of sugar-based nonionic surfactant used as a corrosion inhibitor. The corrosion inhibition efficiencies of polysobates [52] in HCl medium ranged from 83 to 88 %. Overviewing the obtained corrosion inhibition efficiencies of the synthesized inhibitors in Table 3 revealed that the average efficiencies ranged between 60 and 71.8 % at low concentrations. At higher concentrations, the efficiencies ranged between 98.5 and 91 %. Comparison between the corrosion inhibition efficiencies of the synthesized nonionic surfactants V_{1-3} and H_{1-3} and the commercial nonionic corrosion inhibitors showed the satisfactory performance of the former as corrosion inhibitors in acidic media.

Conclusion

The study revealed several points:

1. The surface activities of the synthesized nonionic surfactants depend on their chemical structures.
2. The synthesized surfactants have low emulsification tendency.
3. Thermodynamic data showed that the surfactants tend to adsorb at the solution interface and micellize in bulk of solution spontaneously.
4. Polarization and impedance measurements showed the high efficiency of the synthesized surfactants in acidic medium.
5. The synthesized surfactants exhibit comparable inhibition to commercial nonionic inhibitors.

References

1. Mahdavian M, Tehrani-Begha AR, Holmberg K (2011) Comparison of cationic gemini surfactant and the corresponding monomeric surfactant for corrosion protection of mild steel in hydrochloric acid. J Surfactants Deterg 14:605–613
2. Ajmal M, Rawat J, Quraishi MA (1999) Thioamidines as novel class of corrosion inhibitors. Br Corros J 34:220–226
3. Tawfik SM, Sayed A, Aiad I (2012) Corrosion inhibition by some cationic surfactants in oil fields. J Surfactants Deterg 15:577–585
4. Negm NA, Zaki MF, Said MM, Morsy SM (2011) Inhibitory action of biodegradable modified vanillin on the corrosion of carbon steel in 1 M HCl. Corros Sci 53:4233–4240
5. Pillai K, Narayan R (1978) Inhibition of corrosion of iron in acids by thiourea and derivatives. J Electrochem Soc 125:1393–1402
6. Negm NA, El Farargy AF, Al Sabagh AM, Abdelrahman NR (2011) New Schiff base cationic surfactants: surface and thermodynamic properties and applicability in bacterial growth and metal corrosion prevention. J Surfactants Deterg 14:505–514
7. Kendig MW (2004) US Patent application 20040175587A1
8. Yıldırım A, Ozturk S, Cetin M (2013) Novel amide-based cationic surfactants as efficient corrosion inhibitors for carbon steel in HCl and H2SO4 media. J Surfactants Deterg 16:13–23
9. Negm NA, Zaki MF (2008) Corrosion inhibition efficiency of nonionic Schiff base amphiphiles of p-aminobenzoic acid for aluminum in 4 N HCl. Colloids Surf A 322:97–102
10. El-Etre AY (2001) Inhibition of acid corrosion of aluminum using vanillin. Corros Sci 43:1031–1039
11. Shahidi M, Sasaei E, Ganjehkaviri M, Gholamhosseinzadeh MR (2012) Investigation of vanillin as a green corrosion inhibitor for stainless steel using electrochemical techniques. J Phys Theory Chem 9:149–161
12. Rosliza R, Noraaini A, Wan Nik WB (2010) Study on the effect of vanillin on the corrosion inhibition of aluminum alloy. J Appl Electrochem 40:833–840
13. Kusmierek E, Chrzescijanska E (2015) Tannic acid as corrosion inhibitor for metals and alloys. Mater Corros 66:169–174
14. Antonijevic MM, Petrovic MB (2008) Copper corrosion inhibitors. Int J Electrochem Sci 3:1–28
15. Umoren SM, Obot IB, Ebenso EE, Okafor PC, Ogobe O, Oguzie EE (2006) Gum Arabic as a potential corrosion inhibitor for

16. aluminium in alkaline medium and its adsorption characteristics. Anti Corros Methods Mater 53:277–282
16. El-Etre AY, Abdallah M, El-Tantawy ZE (2005) Corrosion inhibition of some metals using Lawsonia extract. Corros Sci 47:385–395
17. Aiad IA, Negm NA (2009) Some Schiff base surfactants as steel corrosion inhibitors. J Surfactants Deterg 12:313–319
18. Negm NA, Aiad IA (2007) Synthesis and characterization of multifunctional surfactants in oil-field protection applications. J Surfactants Deterg 10:87–92
19. Quraishi MA, Khan MAW, Ajmal M, Muralidharan S, Iyer SV (1997) Influence of heterocyclic anils on corrosion inhibition and hydrogen permeation through mild steel in acid chloride environments. Corrosion 53:475–481
20. Negm NA, Morsy SMI, Said MM (2005) Corrosion inhibition of some novel hydrazone derivatives. J Surfactants Deterg 8:95–98
21. Sayed GH, Ghuiba GM, Abdou MI, Badr EA, Tawfik SM, Negm NA (2011) Synthesis, surface and thermodynamic parameters of some biodegradable nonionic surfactants derived from tannic acid. Colloids Surf A 393(2011):96–104
22. Negm NA, Kandile NG, Aiad IA, Mohammad MA (2011) New eco-friendly environmentally cationic surfactants: synthesis, characterization and applicability as corrosion inhibitors for carbon steel in 1 N HCl. Colloids Surf A 391:224–233
23. Negm NA, Mohamed AS (2008) Synthesis, characterization and biological activity of sugar-based gemini cationic amphiphiles. J Surfactants Deterg 11:215–221
24. Negm NA (2007) Solubilization, surface active and thermodynamic parameters of gemini amphiphiles bearing nonionic hydrophilic spacer. J Surfactants Deterg 8:71–80
25. Negm NA (2005) Zwitterionic surfactants: synthesis, surface and thermodynamic properties of N-ethyl alkanoate-N-ethanol-N-methyl-N-carboxymethyl betaine Egypt. J Petrol 14:1–8
26. John H (1992) Surfactant aggregation, vol 4. Blackie, London
27. Negm NA, Mohamed AS (2004) Surface and thermodynamic properties of diquaternary bola-form amphiphiles containing aromatic spacer. J Surfactants Deterg 7:23–30
28. Zana R (1996) Progress in synthesis in gemini surfactants. Curr Opin Colloid Interface Sci 1:566–572
29. Rosen MJ (1989) Surface and interfacial phenomena, 2nd edn. Wiley, New York, p 151
30. Negm NA, El Farargy AFM, Mohammed DE, Mohamad HN (2015) Environmentally friendly nonionic surfactants derived from tannic acid: synthesis, characterization and surface activity. J Surfactants Deterg 15:433–443
31. Sowada R (1994) The effect of electrolytes on the critical micelle concentration on ionic surfactants. Tenside Surfactants Deterg 31:4–9
32. Bentiss F, Bouanis M, Mernari B, Traisnel M, Vezin H, Lagrenee M (2006) Understanding the adsorption of 4H-1,2,4-triazole derivatives on mild steel surface in molar hydrochloric acid. Appl Surf Sci 253:3696–3703
33. Behpour M, Ghoreishi SM, Salavati-Niasari M, Ebrahimi B (2008) Evaluating two new synthesized S–N Schiff bases on the corrosion of copper in 15 % hydrochloric acid. Mater Chem Phys 107:153–157
34. Negm NA, Al Sabagh AM, Migahed MA, Abdel Bary HM, El Din HM (2010) Effectiveness of some diquaternary ammonium surfactants as corrosion inhibitors for carbon steel in 0.5 M HCl solution. Corros Sci 52:2122–2132
35. Ajmal M, Miden AS, Quraishi MA (1994) 2-Hydrazino-6-methyl-benzothiazole as an effective inhibitor for the corrosion of mild steel in acidic solutions. Corros Sci 36:79–84
36. Asefi D, Arami M, Sarabi AA, Mahmoodi NM (2009) The chain length influence of cationic surfactant and role of nonionic

cosurfactants on controlling the corrosion rate of steel in acidic media. Corros Sci 51:1817–1821

37. El Achouri M, Infante MR, Izquierdo F, Kertit S, Gouttaya HM, Nciri B (2009) Synthesis of some cationic gemini surfactants and their inhibitive effect on iron corrosion in hydrochloric acid medium. Corros Sci 43:19–35

38. Negm NA, Elkholy NA, Zahran MK, Tawfik SM (2010) Corrosion inhibition efficiency and surface activity of surface active benzothiazol-3-ium cationic schiff base derivatives in hydrochloric acid. Corros Sci 52:3523–3536

39. Negm NA, Ghuiba EM, Mahmoud SA, Tawfik SM (2011) Biocidal and anti-corrosive activities of benzoimidazol-3-ium cationic Schiff base surfactants. Eng Life Sci 11:496–510

40. Negm NA, Elkholy NA, Tawfik SM (2011) Corrosion inhibition of carbon steel by some quaternary surface active isoxazol-2-ium cationic Schiff bases in hydrochloric acid solution. Corros Sci 53:3566–3575

41. Negm NA, Badr EA, Aiad IA, Zaki MF, Said MM (2012) Investigation the inhibitory action of novel diquaternary diSchiff bases on the acid dissolution of carbon steel in 1 M hydrochloric acid solution. Corros Sci 65:77–86

42. Negm NA, Kandile NG, Mohammed MA, Bedr EA (2012) Gravimetric and electrochemical evaluation of environmentally friendly nonionic corrosion inhibitors for dissolution of carbon steel in 1 M HCl. Corros Sci 65:94–103

43. Ozcan M, Dehri J, Erbil M (2004) Organic sulphur-containing compounds as corrosion inhibitors for mild steel in acidic media: correlation between inhibition efficiency and chemical structure. Appl Surf Sci 236:155–164

44. Chauhan LR, Gunasekaran G (2007) Corrosion inhibition of mild steel by plant extract in dilute HCl medium. Corros Sci 49:1143–1161

45. Kalman E, Varhegyi B, Felhosi I, Karman FH, Shaban A (1994) Corrosion Inhibition by 1-hydroxy-ethane-1,1-diphosphonic acid: an electrochemical impedance spectroscopy study. J Elecrochem Soc 141:3357–3360

46. Elkadi L, Marnari B, Traisnel M, Bentiss F, Lagrenee M (2000) The inhibition action of 3,6-bis(2-methoxyphenyl)-1,2-dihydro-1,2,4,5-tetrazine on the corrosion of mild steel in acidic media. Corros Sci 42:703–719

47. Quraishi MA, Rawat J (2001) Influence of iodide ions on inhibitive performance of tetraphenyl-dithia-octaaza-cyclotetradeca-hexaene (PTAT) during pickling of mild steel in hot sulfuric acid. Mater Chem Phys 70:95–99

48. Oguzie EE, Li Y, Wang FH (2007) Effect of 2-amino-3-mercaptopropanoic acid (cysteine) on the corrosion behaviour of low carbon steel in sulphuric acid. Electrochim Acta 53:909–914

49. El-Mahdy GA, Atta AM, Al-Lohedan HA (2013) Water soluble nonionic Rosin surfactants as corrosion inhibitor of carbon steel in 1 M HCl. Int J Electrochem Sci 8:5052–5066

50. Shalaby MN, Osman MM (2002) Application of some commercial nonionic surfactants in the field of corrosion inhibition. Mater Corros 53:827–832

51. Abdallah M, El-Etre AY (2013) Corrosion inhibition of nickel in sulfuric acid using tween surfactants. Portug Electrochim Acta 21:315–326

52. Sobhia M, Abdallah M, Hfaeza E (2013) Some polysorbate compounds as corrosion inhibitors for carbon steel in hydrochloric acid. J Adv Chem 5:830–838

Nabel A. Negm received his Ph.D. from Ain Shams University in 2000. He spent 6 months as a research fellow at the Max Planck Institute of Colloids and Surfaces, Golm, Germany; and 2 months as visiting professor at the Indian Institute of Science (IISc), Mechanical Engineering Department, Bangalore, India. He is currently an assistant professor at the Petrochemicals Department of the Egyptian Petroleum Research Institute. He is interested in several surfactants applications, including detergency, emulsification, solubilization, corrosion inhibition of metals, and oil field chemicals. Also, he is interested in the biological activity of surfactants and their metal complexes towards bacteria, fungi, and yeast. His recent R&D has been focused on mixed surfactants and mixed surfactant–protein systems. He is currently an associate editor of *Journal of Surfactants and Detergents* and vice head of the Petrochemicals Department, Egyptian Petroleum Research Institute, Egypt.

Sayed Abdelkader Ahmed is a professor of organic chemistry at the Faculty of Science, Beni Suef University, Egypt.

Emad A. Badr obtained his Ph.D. from Al-Azhar University and is now an assistant professor at the Petrochemicals Department at the Egyptian Petroleum Research Institute, Egypt.

Mona Abdel Ghani is a Ph.D. student in the chemistry department at Beni Suef University, Egypt.

Mohamed Abd El-Raouf obtained his Ph.D. from Al-Azhar University in 2007 and is now a researcher at the Egyptian Petroleum Research Institute, Egypt. His research interests are in corrosion and surfactants applications.